miR-34c-3p regulates PKA activity independent of cAMP via ablation of PRKAR2B in *Theileria annulata*-infected leukocytes and *Plasmodium falciparum*-infected erythrocytes

Malak Haidar[1,2,3], Fathia Ben-Rached[1], Matthias Wagner[4,5], Tobias Mourier[1], Zineb Rchiad[1], Sara Mfarrej[1], Chetan E. Chitnis[4], Arnab Pain[1, 6,7]* and Gordon Langsley[2,3*].

[1]Pathogen Genomics Laboratory, Biological and Environmental Sciences and Engineering (BESE) Division, King Abdullah University of Science and Technology (KAUST), Thuwal-23955-6900, Kingdom of Saudi Arabia.

[2]Inserm U1016, Cnrs UMR8104, Cochin Institute, Paris, 75014 France.

[3]Laboratoire de Biologie Comparative des Apicomplexes, Institut Cochin-Inserm u1016, UMR Cnrs 8104, Faculté de Médecine, Université Paris Descartes - Sorbonne Paris Cité, 75014, France.

[4]Malaria Parasite Biology and Vaccines Unit, Department of Parasites and Insect Vectors, Institut Pasteur, Paris 75015, France.

[5]Université de Paris, Sorbonne Paris Cité, Paris, France"

[6]Global Station for Zoonosis Control, GI-CoRE, Hokkaido University, N20 W10 Kita-ku, Sapporo, Japan

[7]Nuffield Division of Clinical Laboratory Sciences (NDCLS), University of Oxford, Headington, Oxford, OX3 9DU, UK

Corresponding Authors:

Arnab Pain, Pathogen Genomics Laboratory, Biological and Environmental Sciences and Engineering (BESE) Division, King Abdullah University of Science and Technology (KAUST), Thuwal-23955-6900, Kingdom of Saudi Arabia, +966 (0) 2808-256, arnab.pain@kaust.edu.sa

Gordon Langsley, Laboratoire de Biologie Comparative des Apicomplexes, Institut Cochin-Inserm u1016, UMR Cnrs 8104, Faculté de Médecine, Université Paris Descartes - Sorbonne Paris Cité, 75014, France, 33-(0)1-40-51-65-47, gordon.langsley@inserm.fr

Abstract

MicroRNAs (miRNAs) are small non-coding RNAs that can play critical roles in regulating various cellular processes including during many parasitic infections. Here, we report a regulatory role for miR-34c-3p in cAMP-independent regulation of PKA activity in *Theileria annulata* and *Plasmodium falciparum* infections of bovine leukocytes and human erythrocytes, respectively. We identified *prkar2b* (cAMP-dependent protein kinase A type II-beta regulatory subunit), as a novel miR-34c-3p target gene and demonstrated how infection-induced up-regulation of miR-34c-3p in leukocytes repressed PRKAR2B expression to increase PKA activity and promote the virulent disseminating tumour phenotype of *T. annulata*-transformed macrophages. When human erythrocytes are infected by *P. falciparum* they accumulate miR-34c-3p that ablates both *prkar2b* and parasite *Pfpkar* mRNA. However, erythrocytes lack protein translation machinery so only miR-34c-3p-mediated loss of *Pfpkar* transcripts results in an increase in PfPKA kinase activity. Inhibition of miR-34c-3p increases *Pfpkar* expression to reduce PfPKA activity leading to slowing of intra-erythrocyte parasite development and a reduction in invasion of fresh red blood cells. Finally, we demonstrate that miR-34c-3p regulation of *prkar2b* expression is generalizable, by showing that it can negatively regulate *prkar2b* expression and PRKAR2B protein levels in human cancer cell lines and that brown adipose tissue displays high levels of miR-34c-3p and corresponding low levels of *prkar2b* mRNA compared to white adipose tissue. Induction of miR-34c-3p therefore, represents a novel cAMP-independent way of regulating PKA activity in a range of cell types associated with cancer, diabetes and parasitic diseases.

Keywords: miR-34c-3p, PRKAR2B, PKA, *Theileria*, *Plasmodium*

Introduction

MicroRNAs are a class of small non-coding RNAs and are key regulators in several biological processes ranging from development and metabolism to apoptosis and signaling pathways (Ambros, 2004, Bartel, 2004). Indeed, their profiles are altered in many human diseases and particularly in cancer (Alvarez-Garcia and Miska, 2005, Esquela-Kerscher and Slack, 2006), making them a major focus of research. The up- or down-regulation of miRNAs can cause drastic changes to gene expression due to the fact that miRNAs have up to hundreds of potential mRNA targets (Seitz, 2017). Changes to gene expression can lead to malignant transformation, especially if miRNA targets include genes that regulate cell homeostasis, proliferation, cell cycle progression, adhesion, or dissemination (Baranwal and Alahari, 2010).

Post-transcriptional control of gene expression by miRNAs is also increasingly recognized as a central part of host/pathogen interactions. The role of miRNAs in bacterial (Eulalio et al., 2012, Staedel and Darfeuille, 2013), viral (kaCullen, 2011), parasitic helminth (Britton et al., 2014) and protozoan infections is now well established. *Plasmodium* and *Theileria* parasites are obligate intracellular protozoa of the phylum Apicomplexa. The goal for *Plasmodium* and *Theileria* parasites is to infect their invertebrate insect hosts (mosquitoes and ticks, respectively) for successful transmission and continuity of the life cycle with the sexual forms – thus ensuring exchanges of genetic material via genetic recombination. To ensure transmission to blood sucking vectors the parasite population is amplified in the mammalian host. Post-inoculation by the insect vector, sporozoites of both species invade MHC class I- and class II-positive cells (hepatocytes for *Plasmodia* and leukocytes for *Theileria*), but thereafter

their life cycles differ, as the *Theileria* parasite population amplifies within the infected leukocyte. Apicomplexan parasites are able to alter the global gene expression patterns of their respective host cells by interfering with signaling cascades to neutralize host defences (Plattner and Soldati-Favre, 2008) and improve their capacity to infect, proliferate and disseminate. Apicomplexa manipulate their host cell's miRNomes to their own benefit (Cannella et al., 2014, Shapira et al., 2002, Zeiner et al., 2010). We have shown that miR-126-5p by directly targeting and suppressing JNK-Interacting-Protein JIP-2 liberates cytosolic JNK to translocate to the host cell nucleus and phosphorylate c-Jun that trans-activates AP-1-driven transcription of *mmp9* to promote tumour dissemination of *Theileria*-transformed macrophages (Haidar et al., 2018). Moreover, miR-155 is also induced by infection to supress De-Etiolated Homolog 1 expression that diminishes c-Jun ubiquitination (Marsolier et al., 2013). An increase in c-Jun levels leads to an augmentation in *BIC* (pri-miR-155**)** transcripts that contain miR-155, explaining how a positive feedback-loop contributes to the growth and survival of *Theileria*-infected leukocytes (Marsolier et al., 2013). Furthermore, exosomes and their miRNA cargo play an important role in the manipulation of the host cell phenotype and the pathobiology of both *Theileria* and *Plasmodium* infections (Gillan et al., 2019, Mantel et al., 2016). However, in contrast to *Toxoplasma,* the genomes of *T. annulata* and *P. falciparum* lack orthologs of Dicer and Argonaute, crucial enzymes in miRNA biogenesis (Coulson et al., 2004, Hall et al., 2005). Moreover, sequencing and bioinformatics analyses of small RNA libraries from *P. falciparum*-infected erythrocytes did not identify parasite-specific miRNAs (Rathjen et al., 2006). That said, at least 100 different human miRNAs are taken up by the parasite with a particular enrichment of miR-451 and let-7i in parasitized HbAS and HbSS erythrocytes (LaMonte et al., 2012). LaMonte *et al*. confirmed that human miRNA transferred into the parasite formed chimeric fusions with *P.*

falciparum mRNA via impaired ribosomal loading, resulting in translational inhibition, eventually impairing parasite biology and survival. It is not yet known what determines the specific enrichment of particular miRNAs, or its incorporation into specific parasite mRNAs (Cohen et al., 2015, Hall et al., 2005). Extracellular Vesicles (EVs) derived from *P. falciparum*-infected red blood cells (iRBC) contain miRNAs that can modulate target gene expression in recipient host cells and multiple miRNA species in EVs were identified bound to AGO2 forming functional complexes (Mantel et al., 2016). Furthermore, *P. falciparum* takes up micro-vesicles containing AGO2 and miRNA from infected RBCs (Wang et al., 2017).

Infection by *T. annulata* and *P. falciparum* alters the abundance of a number of host cell miRNAs, and herein we functionally characterized the role of miR-34c-3p. We demonstrate that by targeting *prkar2b* coding for the Protein Kinase A type II-beta regulatory subunit, miR-34c-3p regulates mammalian PKA activity independently of cAMP **(**Cyclic Adenosine Monophosphate) in *Theileria*-infected macrophages. Overexpression of miR-34c-3p diminished *prkar2b* transcripts and hence PRKAR2B protein levels and consequently increased PKA activity in attenuated (diminished in dissemination) *Theileria*-transformed macrophages re-establishing their virulent disseminating tumour-like phenotype.

Similarly, we confirmed higher levels of miR-34c-3p in *P. falciparum*-infected red blood cells (iRBC) and demonstrated that inhibition of miR-34c-3p binding to its cognate seed sequence enhanced both erythrocyte *prkar2b* and parasite *Pfpkar* RNA levels, but only parasite PKA activity. Inhibition of miR-34c-3p slowed intra-erythrocyte parasite development and

dampened re-invasion of fresh red blood cells, the latter being consistent with the requirement of PfPKAc for erythrocyte invasion (Dawn et al., 2014, Syin et al., 2001).

Results

miR-34c-3p is differentially expressed in *T. annulata*-infected leukocytes:

T. annulata-transformed macrophages disseminate in infected animals, but upon long-term *in vitro* passaging their virulent virulence capacity to disseminate becomes attenuated and they are used as live vaccines in the control of tropical theileriosis (Darghouth, 2008). miRNome profiles of virulent and attenuated *T. annulata*-transformed macrophages and infected (TBL20) compared to non-infected (BL20) B cells identified miR-34c-3p, as a miRNA upregulated after infection and down-regulated upon attenuation (Haidar et al., 2018). These observations were first confirmed by qRT-PCR (Figure 1A) and transfection of attenuated macrophages with a miR-34c-3p agonist (mimic) increased miR-34c-3p expression (Figure 1B, left panel). Transfection of attenuated macrophages with the miR-34c mimic had no influence on the levels of an irrelevant miRNA (Fig. 1B, right panel).

miR-34c-3p targets PRKAR2B to regulate PKA activity independently of fluxes in cAMP:

Mammalian PKA is a hetero-tetrameric enzyme composed of two catalytic subunits associated with two regulatory subunits. There are four different regulatory subunit genes (R1A, R1B, R2A, and R2B) that exhibit differential expression patterns and play different roles in cell differentiation and growth control (Skalhegg and Tasken, 2000). The catalytic subunit PKA-C is bound to an inhibitory regulatory subunit (PKA-R), but upon binding of cAMP to the regulatory subunits, catalytic subunits are released to act as a serine/threonine kinase in both the cytoplasm

and nucleus to phosphorylate the target proteins. PKA-C substrates include transcription factors and other proteins involved in developmental processes (Johnson et al., 2001).

Using two publicly available miRNA target prediction algorithms (miRWalk (Dweep and Gretz, 2015) and TargetScan (Agarwal et al., 2015)), we searched the *Bos taurus* genome for potential miR-34c-3p target genes. Interestingly, of the 4 genes coding for regulatory subunits of PKA the search identified only *prkar2b*, so we investigated the capacity of miR-34c-3p to impact on dissemination of *T. annulata*-transformed macrophages that we have shown to be PKA-dependent (Dawn et al., 2014, Haidar et al., 2015, Merckx et al., 2008). First, we measured *prkar2b* mRNA levels in virulent and attenuated macrophages and following overexpression of miR-34c-3p in attenuated macrophages (Figure 2A). *Prkar2b* transcripts are more abundant in attenuated macrophages that have lower miR-34c-3p levels (see Fig.1) and PRKAR2B protein levels decreased in attenuated macrophages transfected with the miR-34c-3p mimic (Fig. 2A, middle panel). Moreover, confirmation that *Prkar2b* is a direct miR-34c-3p-target gene came from fusing the 3'-UTR of bovine *prkar2b* containing the miR-34c-3p seed 3´- to the Renilla luciferase translational stop codon. Following transfection of the reporter construct luciferase activity was measured in virulent, attenuated, and attenuated macrophages treated with the miR-34c-3p mimic (Fig.2A, right panel). Due to attenuated macrophages having lower levels of miR-34c-3p they displayed higher luciferase activity than virulent macrophages. Upon mimic treatment the luciferase activity in attenuated macrophages dropped significantly confirming that *prkar2b* is a direct target of miR-34c-3p.

As PKA is known to phosphorylate the transcription factor cAMP response element binding protein (CREB) (Mayr and Montminy, 2001, Rosenberg et al., 2002), the mimic-induced drop in *prkar2b* expression resulted in a corresponding increase in PKA kinase activity and an increase in CRE-driven luciferase (Fig. 2 A&B). Taken together, this demonstrated that mammalian PKA kinase activity can be regulated independent of cAMP via miR-34c-3p-mediated ablation of *prkar2b*.

Changes in miR-34c-3p levels influence dissemination of *T. annulata*-transformed macrophages:

The capacity of virulent macrophages to traverse Matrigel is greater than that of attenuated macrophages and is a reflection the dissemination potential of *T. annulata*-transformed macrophages (Chaussepied et al., 2010). Transfection of attenuated macrophages with the miR-34c-3p mimic restored their capacity to traverse Matrigel to match that of virulent macrophages (Figure 3). This demonstrates one of the ways that infection-induced increase in miR-34c-3p levels contributes to aggressive dissemination of *T. annulata*-transformed virulent macrophages and how a drop in miR-34c-3p levels contributes to the reduced dissemination potential of attenuated macrophages.

miR-34c-3p targets both *prkar2b* and *Pfpkar* to regulate infected erythrocyte PKA activity independently of fluxes in cAMP

Having demonstrated above that changes in miR-34c-3p impacted on PKA activity of *T. annulata*-infected macrophages we searched for miR-34c-3p seed sequences in the single regulatory subunit of parasite PKA. We were unable to detect miR-34c-3p seed sequences in the

T. annulata regulatory subunit (*Tapkar*), but surprisingly noticed the regulatory subunit of *P. falciparum* PKA (*Pfpkar*) harbored a potential miR-34c-3p seed (Figure S1). As erythrocyte infection by *P. falciparum* has been reported to increase miR-34c-3p levels (see supplementary files in (Mantel et al., 2016)) we confirmed that infection does lead to increased amounts of miR-34c-3p and identified the developmental parasite stage the largest increase (Figure 4). *P. falciparum* infection does indeed raise intra-erythrocyte levels of miR-34c-3p and this can be ascribed mostly to intra-erythrocyte ring and merozoite developmental stages (Fig. 4A). Inhibition of miR-34c-3p binding to its cognate seed sequence raised both *prkar2b* and *Pfpkar* transcript levels (Fig. 4B).

Inhibition of miR-34c-3p increases *P. falciparum*-infected erythrocyte PKA kinase activity and slows parasite development:

Although erythrocytes harbor PRKAR2B they no longer have the machinery to translate residual *prkar2b* transcripts into protein (Gautier et al., 2016, Gautier et al., 2018) meaning that the miR-34c-3p-induced drop in *prkar2b* mRNA can't result in reduced PRKAR2B protein. By contrast *P. falciparum* can translate mRNA into protein, so upon inhibition of miR-34c-3p the rise in *Pfpkar* transcripts results in increased PfPKAr protein and reduced PKA kinase activity of infected red blood cells (Figure 5A). Culture of infected erythrocytes was synchronized at the schizont stage and then following merozoite invasion of fresh red blood cells ring-infected erythrocytes were treated with the miR-34c-3p inhibitor and the percentage of the different developmental stages were monitored (Fig. 5B). Inhibition of miR-34c-3p that dampens PKA activity slowed parasite intra-erythrocytic development such that at 64 h inhibitor treated parasites were still at the ring stage, whereas trophozoites could be readily detected in non-

treated red blood cells (Fig. 5B). As miR-34c-3p levels are highest in merozoite-infected red blood cells (Fig. 4A), a re-invasion assay was performed (for gating strategy see Figure S2) using both miR-34c-3p mimic and inhibitor treated infected erythrocytes. Mimic treatment increased the number of freshly invaded ring stage parasites by 10% and conversely inhibitor treatment similarly reduced the number of ring-infected red blood cells (Fig. 5C). To confirm that this was due to miR-34c-3p-targeting of *pfpkar* transcripts the re-invasion assay was repeated using transgenic parasites that overexpress *pfpkar* (Merckx et al., 2008). The abundance of *pfpkar* transcripts expressed by transgenic parasites markedly diminished the impact of miR-34c-3p mimic and inhibitor treatment on parasite intraerythrocyte development (Fig. 5D).

Discussion

We've shown that miR-34c-3p-induced loss of PRKAR2B enhanced PKA activity to induce CREB transactivation that are important contributors to *Theileria*-transformed macrophage dissemination. By contrast, in attenuated macrophages levels of miR-34c-3p are low and consequently PRKAR2B remains high sequestering more catalytic subunit into inactive complexes leading to dampened Matrigel traversal. We have previously described how TGF-β secreted by *T. annulata*-transformed macrophages contributes to sustaining PKA activity in virulent macrophages via PGE2 engagement of EP4 to augment levels of cAMP (Haidar et al., 2015). Now, we provide an infection-induced epigenetic mechanism for regulating host cell PKA activity independent of fluxes in cAMP. In *T. annulata*-transformed macrophages infection targets host cell PKA activity in 3 different ways; 1) by raising cAMP levels (Haidar et al., 2015); 2) by suppressing the endogenous inhibitor PKIG (Haidar et al., 2015) and 3) by miR-34c-3p ablation of PRKAR2B subunit expression and this three-pronged "attack" underscores

the key role PKA plays in dissemination of *T. annulata*-transformed macrophages.

MicroRNAs are known to target many different genes and miR-34c-3p is no exception, since we were able to identify its seed sequences in just over 100 bovine genes whose expression is down-regulated in virulent macrophages, where miR-34c-3p levels are high, and whose expression increases in attenuated macrophages, where miR-34c-3p levels are low (Table S1). Just how many of the 100 genes are actually targeted by miR-34c-3p is difficult to say, as is whether ablation of a gene other than *prkar2b* contributes to the phenotype we observe upon miR-34c-3p mimic or antagonist treatment. That said, we've demonstrated that the seed sequence in *prkar2b* is a bona fide miR-34c-3p target and that mimic treatment of attenuated macrophages decreases PRKAR2B protein levels, increases PKA activity and Matrigel traversal, traits we have previously ascribed to heighten cAMP-dependent PKA (Haidar et al., 2015).

Since mature erythrocytes lose their nuclei during erythropoiesis, a conventional belief has been that red blood cells do not contain any nucleic acid. However, several independent groups have described that human erythrocytes contain abundant miRNAs that persist beyond terminal differentiation (Azzouzi et al., 2015, Chen et al., 2015, Neuman et al., 2015). Herein, we showed that miR-34c-3p can ablate *Pfpkar* transcripts in contrast to *Tapkar* that lacks a miR-34c-3p seed sequence. The N-terminus of *Pfpkar* is extended and quite different to the regulatory subunits of other Apicomplexa (Haste et al., 2012) and is only conserved in higher ape malaria parasites (Figure S3). We confirmed the supplementary data in (Mantel et al., 2016) that miR-34c-3p levels are higher in RBC-infected with *P. falciparum* than in non-infected erythrocytes. Although red blood cell miR-34c-3p targets were not previously characterized we now show that

the amount of red blood cell *prkar2b* mRNA in infected erythrocytes increases upon treatment with the miR-34c-3p antagonist. Thus, both *T. annulata* infection of leukocytes and *P. falciparum* infection of erythrocytes lead to increased miR-34c-3p levels and consequent ablation of *prkar2b* transcripts. However, unlike leukocytes, erythrocytes lack both transcription and the protein translation machinery to convert changes in the amount of residual *prkar2b* transcripts into alterations in PRKAR2B protein levels. Differently to *T. annulata* infection of leukocytes, increased amounts of miR-34c-3p in *P. falciparum*-infected erythrocytes dampens the amount of *pfpkar* transcripts resulting in increased parasite PKA kinase activity. To ascribe these changes to miR-34c-3p-mediated ablation of *pfpka* transcripts we treated transgenic parasites over-expressing the regulatory subunit (Merckx et al., 2008) and indeed, the slower parasite development phenotype was a less marked due to transgenic parasites expressing an abundance of *Pfpkar* transcripts. Parasite cAMP-dependent PKA activity is known to be high in merozoites (Dawn et al., 2014) and crucial for their invasion of red blood cells (Patel et al., 2019) and consistently inhibition of miR-34c-3p that provoked a drop in PKA kinase activity also provoked reduced invasion efficiency. Genetic inactivation of *pfpkac* did not lead to an obvious slowing of intraerythrocyte parasite development in the first 48 h, and given the crucial role *pfpkac* plays in merozoite invasion subsequent rounds of intraerythrocyte parasite development couldn't be observed (Patel et al., 2019). In contrast, the miR-34c-3p-mediated change in PKA activity and 10% drop in invasion efficiency resulted in a slowing of intraerythrocyte parasite development becoming obvious at 64 h and more evident at 93 h i.e. only after completion of a second round of parasite development in fresh red blood cells. The miR-34c-3p-provoked 10% increase in invasion efficiency. This phenotypic effect, although

small, could over time have a profound fitness benefit on infection outcome (Dhingra et al., 2019).

Besides the novel role miR-34c-3p plays in parasite diseases we also provided evidence that it has the potential to play a similar role in human cancer and obesity. Overexpression of miR-34c-3p decreased *prkar2b* mRNA and corresponding protein levels in two human cancer cell lines (HCT116: human colon cancer cell line and HL-60: human leukemia cell line) and miR-34c-3p levels are higher in brown adipocytes (BAT) compared to white adipocytes (WAT; Fig. S4). This suggests that miR-34c-3p mimics and antagonists could have therapeutic use in the treatment of obesity and cancer, as well as parasite diseases. In summary, in the figure 6 we schematically represent how miR-34c-3p can regulate PKA kinase activity independent of fluxes in cAMP via its ablation of mammalian PRKAR2B.

Materials and Methods

Cell culture: Cells used in this study are *T. annulata*-transformed Ode macrophages, where virulent macrophages used corresponds to passage 62 and attenuated macrophages to passage 364 (Singh et al., 2001). Non-infected BL20 and *T. annulata*-infected BL20 (TBL20) cells used have been previously characterized (Moreau et al., 1999, Theilen et al., 1968). All cells were incubated at 37°C with 5% CO_2 in Roswell Park Memorial Institute medium (RPMI) supplemented with 10% Fetal Bovine Serum (FBS), 2mM L-Glutamine, 100 U penicillin, 0.1mg/ml streptomycin, and 4-(2-hydroxyethyl)-1-piperazineethanesulfonic acid (HEPES) and 5% 2-mercapthoethanol for BL20 and TBL20.

Parasite culturing: *P. falciparum* 3D7 and PfPKAr transgenic parasites (pHL-DHFR-PfPKAr,(Merckx et al., 2008)) were cultured in RPMI 1640 (Life Technologies, 51800-035) supplemented with 0.5% (w/v) Albumax II (11021-29), 200 µM hypoxanthine, 20 µg/mL gentamycin (complete RPMI 1640 medium) in human erythrocytes at a hematocrit between 2.5% and 5%. Parasite cultures were maintained under low oxygen pressure (1% O_2, 3% CO_2, 96% N_2) at 37°C.

RNA extractions: Total RNA of *Theileria*-infected leukocytes and *Plasmodium*-infected erythrocytes were isolated using the Direct-zol RNA Kit (Zymo Research # R2070) and total RNA designated for miRNA experiments was extracted using the mirVana miRNA isolation kit (Thermo Fisher) according to the manufacturer's instructions. The quality of extracted RNA was verified using a Bioanalyzer 2100 and quantification carried using Qubit (Invitrogen, catalogue number Q10210).

qRT-PCR for miRNAs: RNA extracted with the mirVana kit was used. cDNA was synthesized using the TaqMan microRNA RT kit (Applied Biosystems) following the manufacturer's instructions. A total of 10 ng of RNA was used in the reverse transcription reaction with miRNA-specific primers. The real-time reactions were performed in a 7500 HT Fast Real-time PCR system (Applied Biosystems). Data was analysed using the $2^{-\Delta\Delta CT}$. The cycle threshold (Ct) values from the selected miRNA targets were subtracted from the Ct values of the endogenous small noncoding RNA control RNU6B (control miRNA assay; Applied Biosystems).

qRT-PCR for mRNA: Total RNA was reverse transcribed using the High Capacity cDNA Reverse Transcription Kit (Applied biosystems, catalogue number 4368814) as follows: 1 μg of

total RNA, 2 μL of RT buffer, 0.8 μL of 100mM dNTP mix, 2.0 μL of 10X random primers, 1 μL of MultiScribe reverse transcriptase and Nuclease-free water to a final volume of 20 μL. The reaction was incubated 10 min at 25°C, 2 h at 37°C then the enzyme inactivated at 85°C for 5 min. Real time PCR was performed in a 20 μL reaction containing cDNA template, 10 μL 2X Fast SYBR Green Master Mix and 500 nM of forward and reverse primers. The reaction was run on the 7500 HT Fast Real-Time PCR System (Applied Biosystems). GAPDH was used as a housekeeping gene and the results were analyzed by the $2^{-\Delta\Delta CT}$ method. The error bars represent the SEM of 3 biological replicates.

Western Blotting: Cells were harvested and extracted by 1x mammalian lysis buffer (Abcam # ab179835) supplemented with protease and phosphatase inhibitor cocktail (#78440, Thermo Fisher). Protein concentration was determined by the Bradford protein assay. Cell lysates were subjected to Western blot analysis using conventional SDS/PAGE and protein transfer to nitrocellulose filters (Protran, Whatman). The membrane was blocked by 5% non-fat milk-TBST (for anti-PRKAR2B and anti-GAPDH), or 3% non-fat milk-PBST (for anti-actin antibody) overnight at 4 ^{0}C. Antibodies used in immunoblotting were as follows: rabbit polyclonal antibody anti-GAPDH (Merck Millipore #ABS16), mouse monoclonal antibody anti-PRKAR2B (#610625, BD transduction laboratories) and goat polyclonal antibody anti-actin (Santa Cruz Biotechnologies I-19). After washing, proteins were visualized with ECL western blotting detection reagents (Thermo Scientific) with fusion instrument. The β-actin was used as a loading control throughout all experiments.

Matrigel Chamber assay: The invasive capacity of Ode macrophages was assessed *in vitro* by using Matrigel migration chambers, as described (Lizundia et al., 2006). The Culture Coat Medium BME (basement membrane extract) 96-well cell invasion assay was performed according to Culturex instructions (catalog number 3482-096-K). After 24 h of incubation at 37°C, each well of the top chamber was washed once in buffer. The top chamber was placed back onto the receiver plate. 100µL of cell dissociation solution-Calcein AM was added to the bottom chamber of each well, and the mixtures were incubated at 37°C for 1 h with fluorescently labelled cells to dissociate the cells from the membrane before reading at 485-nm excitation and 520-nm emission wavelengths, using the same parameters as those used for the standard curve.

Transfection: Macrophages were transfected by electroporation using the Nucleofector system (Amaxa Biosystems). A, total of 5×10^5 cells was suspended in 100 µL of Nucleofector solution mix with 400pM of mimic of miR-34c-3p (m) and subjected to electroporation using the cell line-specific program T-O17 for *Theileria*-infected macrophages. After transfection, cells were suspended in fresh complete medium and incubated at 37°C with 5% CO_2 for 48 h.

Synchronization of parasite culture and pharmacological inhibition or stimulation of miR-34c-3p: Parasites were cultured to at least 10% parasitemia in T-75 flasks containing 25 mL medium at 2% hematocrit. Parasites were synchronized first at ring stage with two rounds of 5% sorbitol. When most of the parasites had matured to schizonts, the culture was loaded on 70% Percoll cushion and centrifuged for 10 min at 800x g. Schizonts from the top of 70% Percoll were collected washed two times with complete media and re-suspended in complete medium. Parasitemia was adjusted to 0.2-0.5% and 2% hematocrit and the culture was distributed in

triplicates in 6-wells plate with various treatments: 400pM of the mimic (HMI0513-5NMOL, Sigma) or 400pM of the inhibitor (cat# 4464084, ID: MH12342, Ambion from Thermo fisher). The culture was incubated at 37°C with 5% CO_2/3% O_2/balanced N_2 gas mixture, for 96 h. To follow growth, blood smears were prepared and stained with Giemsa solution (Sigma). Parasite stage composition was estimated by counting at least 1000 cells per condition. As a negative control, non-treated cultures were assayed. The total parasitemia was an arithmetic sum of rings, trophozoites, and schizonts at each time point.

Flow cytometry assay for monitoring malaria parasite development: To assess the effect of miR-34c-3p on *P. falciparum* growth, a tightly synchronous 3D7 parasite culture with 0.05% parasitemia at schizont stage was cultured in cRPMI medium with or without 25nM of miR-34c-3p Mimic, miR-34c-3p Inhibitor, or the unrelated miR-155 inhibitor (all solved in water at 20µM according to the manufacturer's protocol) at 37°C, 5% CO_2 and 5% O_2 in a 24-well plate. The haematocrit was adjusted to 0.2% (1:20 dilution from 4%) and the medium was changed every other day. Each condition was cultured in triplicates and repeated with three different biological replicates. The cultures were measured by flow cytometry every 24 h at the time of egress/re-invasion or late ring/early trophozoites stage. For flow cytometric measurement, 200 µL of the diluted culture was transferred to a 96-well round bottom plate. To this dilution, 5 mL of 200× SYBR Green (diluted in PBS) was added to a final concentration of 5× SYBR Green. The plate was then incubated for 30 min at 37°C, 5% O_2 and 5% CO_2 in the dark. Samples were measured on a calibrated MACSquant flow cytometer on the FSC and B1 fluorescent channel (λ_{Ex} 488 nm, λ_{Em} 525/50 nm). Obtained flow cytometric data was assessed with the FlowJo 10 Software (FlowJo, LLC). The gating strategy is shown in Appendix S4. Briefly, after gating for singlets,

we excluded debris, merozoites and cells bigger than RBC. In a third step, gates for rings, trophozoites and multiply infected iRBC, and schizonts were set up. The correct alignment of the gates was controlled by Giemsa stained smears. The parasitemia was defined as the sum of the three aforementioned gates. Relative re-invasion was calculated as the percentage of rings in the condition divided by the percentage of rings in the control.

CREB luciferase assay: After transfection, cells were suspended in fresh complete medium and incubated at 37°C, 5% CO_2 for 24 h and cells were lysed after 48 h post transfections. Measurements of luciferase and β-galactosidase activities were performed using the Dual Light Assay system (Life Technologies) and luminometer Centro LB 960 (Berthold) according to the manufacturer's instructions.

Measurement of PKA activity: *Theileria*-infected macrophages were transfected with the specific mimic of miR-34c-3p. Samples were then collected, centrifuged at 1500rpm for 5 min and lysed by recommended lysis buffer [20mM MOPS, 50mM β-glycerolphosphate, 50mM sodium fluoride, 1mM sodium vanadate, 5mM EGTA, 2mM EDTA, 1% NP40, 1mM dithiothreitol (DTT), 1mM benzamidine, 1mM phenylmethane-sulphonylfluoride (PMSF) and 10µg/mL leupeptin and aprotinin. For permeabilization of *P. falciparum*-infected red blood cells, Streptolysin O (SLO, Sigma) was first titrated by re-suspending SLO (25000 units) in 5 mL of PBS (10mM sodium phosphate buffer and 145mM NaCl, pH 7,4) containing 0,1 % BSA and activating by incubation with 5-10 mM dithiothreitol at 37°C for 2 h. iRBCs were re-suspended in 200µL of RPMI containing 3-4 hemolytic units of SLO, resulting in hemoglobin release of more than 98%. Following permeabilization with SLO, cells were centrifuged and

washed with 200µL of RPMI. *P. falciparum*-infected erythrocytes pellets were lysed by the recommended buffer and lysates were cleared by centrifugation (15,000 rpm for 15 min at 4°C), and the total amount of proteins in the supernatant was measured by a Bio-Rad protein assay, based on the method of Bradford, using BSA as a standard. PKA activity was measured using an ELISA kit (PKA kinase activity kit, Abcam 139435) according to the manufacturer's instructions.

Statistical Analysis: Data were analysed with the Student's two-tailed T-tests with at least N = 3 for each experiment. All values are expressed as mean+/-SEM. In each figure, the following symbols represent respective p-value ranges: *:P<0.05; **: p<0.005, ***: p < 0.001.

Acknowledgments:

This study was supported by a Competitive Research Grant from the Office for Sponsored Research (OSR-2015-CRG4-2610) at King Abdullah University of Science and Technology (KAUST) awarded to AP and GL.

MH, FBR, SM, TM acknowledge KAUST faculty baseline funding (BAS/1/1020-01-01) to AP. ZR was funded by a Competitive Research Grant from the Office for Sponsored Research (CRG6 URF/1/3392-01 project) KAUST awarded to AP. GL also acknowledges ANR-11-LABX-0024 and core support from INSERM and the CNRS. Work in the laboratory of CC was supported in part by a grant from Agence Nationale de la Recherche (ANR-17-CE15-0010) and internal funds from Institut Pasteur. and MW is part of the Pasteur - Paris University (PPU) International PhD Program. This project has received funding from the European Union's Horizon 2020 research and innovation program under the Marie Sklodowska-Curie grant agreement No 665807.

Author contribution:

AP and GL conceived and designed the study. MH and SM ran and analyzed qRT-PCR reactions, MH performed all biochemical experiments, FBR and MW performed the intra-erythrocytic development of malaria parasite development assays and TM performed bioinformatic analysis. ZR prepared the ssRNAseq libraries that led to the identification of miR-34c. MH prepared the figures and prepared the first draft of the manuscript that was then edited by CC, AP and GL.

Declaration of interests:

The authors declare no competing interests.

References

AGARWAL, V., BELL, G. W., NAM, J. W. & BARTEL, D. P. 2015. Predicting effective microRNA target sites in mammalian mRNAs. *Elife,* 4.

ALVAREZ-GARCIA, I. & MISKA, E. A. 2005. MicroRNA functions in animal development and human disease. *Development,* 132**,** 4653-62.

AMBROS, V. 2004. The functions of animal microRNAs. *Nature,* 431**,** 350-5.

AZZOUZI, I., MOEST, H., WOLLSCHEID, B., SCHMUGGE, M., EEKELS, J. J. M. & SPEER, O. 2015. Deep sequencing and proteomic analysis of the microRNA-induced silencing complex in human red blood cells. *Exp Hematol,* 43**,** 382-392.

BARANWAL, S. & ALAHARI, S. K. 2010. miRNA control of tumor cell invasion and metastasis. *Int J Cancer,* 126**,** 1283-90.

BARTEL, D. P. 2004. MicroRNAs: genomics, biogenesis, mechanism, and function. *Cell,* 116**,** 281-97.

BRITTON, C., WINTER, A. D., GILLAN, V. & DEVANEY, E. 2014. microRNAs of parasitic helminths - Identification, characterization and potential as drug targets. *Int J Parasitol Drugs Drug Resist,* 4**,** 85-94.

CANNELLA, D., BRENIER-PINCHART, M. P., BRAUN, L., VAN ROOYEN, J. M., BOUGDOUR, A., BASTIEN, O., BEHNKE, M. S., CURT, R. L., CURT, A., SAEIJ, J. P., SIBLEY, L. D., PELLOUX, H. & HAKIMI, M. A. 2014. miR-146a and miR-155 delineate a MicroRNA fingerprint associated with Toxoplasma persistence in the host brain. *Cell Rep,* 6**,** 928-37.

CHAUSSEPIED, M., JANSKI, N., BAUMGARTNER, M., LIZUNDIA, R., JENSEN, K., WEIR, W., SHIELS, B. R., WEITZMAN, J. B., GLASS, E. J., WERLING, D. &

LANGSLEY, G. 2010. TGF-b2 induction regulates invasiveness of Theileria-transformed leukocytes and disease susceptibility. *PLoS Pathog,* 6**,** e1001197.

CHEN, T., HAO, Y. J., ZHANG, Y., LI, M. M., WANG, M., HAN, W., WU, Y., LV, Y., HAO, J., WANG, L., LI, A., YANG, Y., JIN, K. X., ZHAO, X., LI, Y., PING, X. L., LAI, W. Y., WU, L. G., JIANG, G., WANG, H. L., SANG, L., WANG, X. J., YANG, Y. G. & ZHOU, Q. 2015. m(6)A RNA methylation is regulated by microRNAs and promotes reprogramming to pluripotency. *Cell Stem Cell,* 16**,** 289-301.

COHEN, A., COMBES, V. & GRAU, G. E. 2015. MicroRNAs and Malaria - A Dynamic Interaction Still Incompletely Understood. *J Neuroinfect Dis,* 6.

COULSON, R. M., HALL, N. & OUZOUNIS, C. A. 2004. Comparative genomics of transcriptional control in the human malaria parasite Plasmodium falciparum. *Genome Res,* 14**,** 1548-54.

DARGHOUTH, M. A. 2008. Review on the experience with live attenuated vaccines against tropical theileriosis in Tunisia: considerations for the present and implications for the future. *Vaccine,* 26 Suppl 6**,** G4-G10.

DAWN, A., SINGH, S., MORE, K. R., SIDDIQUI, F. A., PACHIKARA, N., RAMDANI, G., LANGSLEY, G. & CHITNIS, C. E. 2014. The central role of cAMP in regulating Plasmodium falciparum merozoite invasion of human erythrocytes. *PLoS Pathog,* 10**,** e1004520.

DHINGRA, S. K., GABRYSZEWSKI, S. J., SMALL-SAUNDERS, J. L., YEO, T., HENRICH, P. P., MOK, S. & FIDOCK, D. A. 2019. Global Spread of Mutant PfCRT and Its Pleiotropic Impact on Plasmodium falciparum Multidrug Resistance and Fitness. *mBio,* 10.

DWEEP, H. & GRETZ, N. 2015. miRWalk2.0: a comprehensive atlas of microRNA-target interactions. *Nat Methods,* 12**,** 697.

ESQUELA-KERSCHER, A. & SLACK, F. J. 2006. Oncomirs - microRNAs with a role in cancer. *Nat Rev Cancer,* 6**,** 259-69.

EULALIO, A., SCHULTE, L. & VOGEL, J. 2012. The mammalian microRNA response to bacterial infections. *RNA Biol,* 9**,** 742-50.

GAUTIER, E. F., DUCAMP, S., LEDUC, M., SALNOT, V., GUILLONNEAU, F., DUSSIOT, M., HALE, J., GIARRATANA, M. C., RAIMBAULT, A., DOUAY, L., LACOMBE, C., MOHANDAS, N., VERDIER, F., ZERMATI, Y. & MAYEUX, P. 2016. Comprehensive Proteomic Analysis of Human Erythropoiesis. *Cell Rep,* 16**,** 1470-1484.

GAUTIER, E. F., LEDUC, M., COCHET, S., BAILLY, K., LACOMBE, C., MOHANDAS, N., GUILLONNEAU, F., EL NEMER, W. & MAYEUX, P. 2018. Absolute proteome quantification of highly purified populations of circulating reticulocytes and mature erythrocytes. *Blood Adv,* 2**,** 2646-2657.

GILLAN, V., SIMPSON, D. M., KINNAIRD, J., MAITLAND, K., SHIELS, B. & DEVANEY, E. 2019. Characterisation of infection associated microRNA and protein cargo in extracellular vesicles of Theileria annulata infected leukocytes. *Cell Microbiol,* 21**,** e12969.

HAIDAR, M., ECHEBLI, N., DING, Y., KAMAU, E. & LANGSLEY, G. 2015. Transforming growth factor beta2 promotes transcription of COX2 and EP4, leading to a prostaglandin E2-driven autostimulatory loop that enhances virulence of Theileria annulata-transformed macrophages. *Infect Immun,* 83**,** 1869-80.

HAIDAR, M., RCHIAD, Z., ANSARI, H. R., BEN-RACHED, F., TAJERI, S., LATRE DE LATE, P., LANGSLEY, G. & PAIN, A. 2018. miR-126-5p by direct targeting of JNK-interacting protein-2 (JIP-2) plays a key role in Theileria-infected macrophage virulence. *PLoS Pathog,* 14**,** e1006942.

HALL, N., KARRAS, M., RAINE, J. D., CARLTON, J. M., KOOIJ, T. W., BERRIMAN, M., FLORENS, L., JANSSEN, C. S., PAIN, A., CHRISTOPHIDES, G. K., JAMES, K., RUTHERFORD, K., HARRIS, B., HARRIS, D., CHURCHER, C., QUAIL, M. A., ORMOND, D., DOGGETT, J., TRUEMAN, H. E., MENDOZA, J., BIDWELL, S. L., RAJANDREAM, M. A., CARUCCI, D. J., YATES, J. R., 3RD, KAFATOS, F. C., JANSE, C. J., BARRELL, B., TURNER, C. M., WATERS, A. P. & SINDEN, R. E. 2005. A comprehensive survey of the Plasmodium life cycle by genomic, transcriptomic, and proteomic analyses. *Science,* 307**,** 82-6.

HASTE, N. M., TALABANI, H., DOO, A., MERCKX, A., LANGSLEY, G. & TAYLOR, S. S. 2012. Exploring the Plasmodium falciparum cyclic-adenosine monophosphate (cAMP)-dependent protein kinase (PfPKA) as a therapeutic target. *Microbes Infect,* 14**,** 838-50.

JOHNSON, D. A., AKAMINE, P., RADZIO-ANDZELM, E., MADHUSUDAN, M. & TAYLOR, S. S. 2001. Dynamics of cAMP-dependent protein kinase. *Chem Rev,* 101**,** 2243-70.

KACULLEN, B. R. 2011. Viruses and microRNAs: RISCy interactions with serious consequences. *Genes Dev,* 25**,** 1881-94.

LAMONTE, G., PHILIP, N., REARDON, J., LACSINA, J. R., MAJOROS, W., CHAPMAN, L., THORNBURG, C. D., TELEN, M. J., OHLER, U., NICCHITTA, C. V., HAYSTEAD, T. & CHI, J. T. 2012. Translocation of sickle cell erythrocyte microRNAs into Plasmodium falciparum inhibits parasite translation and contributes to malaria resistance. *Cell Host Microbe,* 12**,** 187-99.

LIZUNDIA, R., CHAUSSEPIED, M., HUERRE, M., WERLING, D., DI SANTO, J. P. & LANGSLEY, G. 2006. c-Jun NH2-terminal kinase/c-Jun signaling promotes survival and metastasis of B lymphocytes transformed by Theileria. *Cancer Res,* 66**,** 6105-10.

MANTEL, P. Y., HJELMQVIST, D., WALCH, M., KHAROUBI-HESS, S., NILSSON, S., RAVEL, D., RIBEIRO, M., GRURING, C., MA, S., PADMANABHAN, P., TRACHTENBERG, A., ANKARKLEV, J., BRANCUCCI, N. M., HUTTENHOWER, C., DURAISINGH, M. T., GHIRAN, I., KUO, W. P., FILGUEIRA, L., MARTINELLI, R. & MARTI, M. 2016. Infected erythrocyte-derived extracellular vesicles alter vascular function via regulatory Ago2-miRNA complexes in malaria. *Nat Commun,* 7**,** 12727.

MARSOLIER, J., PINEAU, S., MEDJKANE, S., PERICHON, M., YIN, Q., FLEMINGTON, E., WEITZMAN, M. D. & WEITZMAN, J. B. 2013. OncomiR addiction is generated by a miR-155 feedback loop in Theileria-transformed leukocytes. *PLoS Pathog,* 9**,** e1003222.

MAYR, B. & MONTMINY, M. 2001. Transcriptional regulation by the phosphorylation-dependent factor CREB. *Nat Rev Mol Cell Biol,* 2**,** 599-609.

MERCKX, A., NIVEZ, M. P., BOUYER, G., ALANO, P., LANGSLEY, G., DEITSCH, K., THOMAS, S., DOERIG, C. & EGEE, S. 2008. Plasmodium falciparum regulatory subunit of cAMP-dependent PKA and anion channel conductance. *PLoS Pathog,* 4**,** e19.

MOREAU, M. F., THIBAUD, J. L., MILED, L. B., CHAUSSEPIED, M., BAUMGARTNER, M., DAVIS, W. C., MINOPRIO, P. & LANGSLEY, G. 1999. Theileria annulata in CD5(+) macrophages and B1 B cells. *Infect Immun,* 67**,** 6678-82.

NEUMAN, R., HAYEK, S., RAHMAN, A., POOLE, J. C., MENON, V., SHER, S., NEWMAN, J. L., KARATELA, S., POLHEMUS, D., LEFER, D. J., DE STAERCKE, C., HOOPER, C., QUYYUMI, A. A. & ROBACK, J. D. 2015. Effects of storage-aged red blood cell transfusions on endothelial function in hospitalized patients. *Transfusion,* 55**,** 782-90.

PATEL, A., PERRIN, A. J., FLYNN, H. R., BISSON, C., WITHERS-MARTINEZ, C., TREECK, M., FLUECK, C., NICASTRO, G., MARTIN, S. R., RAMOS, A., GILBERGER, T. W., SNIJDERS, A. P., BLACKMAN, M. J. & BAKER, D. A. 2019. Cyclic AMP signalling controls key components of malaria parasite host cell invasion machinery. *PLoS Biol,* 17**,** e3000264.

PLATTNER, F. & SOLDATI-FAVRE, D. 2008. Hijacking of host cellular functions by the Apicomplexa. *Annu Rev Microbiol,* 62**,** 471-87.

RATHJEN, T., NICOL, C., MCCONKEY, G. & DALMAY, T. 2006. Analysis of short RNAs in the malaria parasite and its red blood cell host. *FEBS Lett,* 580**,** 5185-8.

ROSENBERG, D., GROUSSIN, L., JULLIAN, E., PERLEMOINE, K., BERTAGNA, X. & BERTHERAT, J. 2002. Role of the PKA-regulated transcription factor CREB in development and tumorigenesis of endocrine tissues. *Ann N Y Acad Sci,* 968**,** 65-74.

SEITZ, H. 2017. Issues in current microRNA target identification methods. *RNA Biol,* 14**,** 831-834.

SHAPIRA, S., SPEIRS, K., GERSTEIN, A., CAAMANO, J. & HUNTER, C. A. 2002. Suppression of NF-kappaB activation by infection with Toxoplasma gondii. *J Infect Dis,* 185 Suppl 1**,** S66-72.

SINGH, S., KHATRI, N., MANUJA, A., SHARMA, R. D., MALHOTRA, D. V. & NICHANI, A. K. 2001. Impact of field vaccination with a Theileria annulata schizont cell culture vaccine on the epidemiology of tropical theileriosis. *Vet Parasitol,* 101**,** 91-100.

SKALHEGG, B. S. & TASKEN, K. 2000. Specificity in the cAMP/PKA signaling pathway. Differential expression,regulation, and subcellular localization of subunits of PKA. *Front Biosci,* 5**,** D678-93.

STAEDEL, C. & DARFEUILLE, F. 2013. MicroRNAs and bacterial infection. *Cell Microbiol,* 15**,** 1496-507.

SYIN, C., PARZY, D., TRAINCARD, F., BOCCACCIO, I., JOSHI, M. B., LIN, D. T., YANG, X. M., ASSEMAT, K., DOERIG, C. & LANGSLEY, G. 2001. The H89 cAMP-dependent protein kinase inhibitor blocks Plasmodium falciparum development in infected erythrocytes. *Eur J Biochem,* 268**,** 4842-9.

THEILEN, G. H., RUSH, J. D., NELSON-REES, W. A., DUNGWORTH, D. L., MUNN, R. J. & SWITZER, J. W. 1968. Bovine leukemia: establishment and morphologic characterization of continuous cell suspension culture, BL-1. *J Natl Cancer Inst,* 40**,** 737-49.

WANG, Z., XI, J., HAO, X., DENG, W., LIU, J., WEI, C., GAO, Y., ZHANG, L. & WANG, H. 2017. Red blood cells release microparticles containing human argonaute 2 and miRNAs to target genes of Plasmodium falciparum. *Emerg Microbes Infect,* 6**,** e75.

ZEINER, G. M., NORMAN, K. L., THOMSON, J. M., HAMMOND, S. M. & BOOTHROYD, J. C. 2010. Toxoplasma gondii infection specifically increases the levels of key host microRNAs. *PLoS One,* 5**,** e8742.

Figure Legends :

Figure 1: miR-34c-3p is differentially expressed in *T. annulata*-infected leukocytes A left. miR-34c-3p levels in uninfected B lymphocytes (BL20) and levels increase when BL20 are infected with *T. annulata* (TBL20). **A right.** Levels of miR-34c-3p are high in virulent macrophages and decrease in attenuated macrophages. **B left panel**. miR-34c-3p levels in attenuated macrophages increase following their transfection with miR-34c-3p mimic. **B right panel**. Transfection of attenuated macrophages with the miR-34c-3p mimic specifically augments only miR-34c-3p levels, since amounts of miR-30f in attenuated macrophages are unaltered following transfection of the miR-34c-3p mimic. Data represent mean ±SEM. n=3. ***P < 0.001 compared to V; ###P < 0.001 compared to A. V stands for virulent, A for attenuated, Am: attenuated transfected with miR-34c mimic.

Figure 2: miR-34c-3p-induced drop in PRKAR2B upregulates PKA kinase activity of *T. annulata*-infected macrophages. A. *Theileria*-transformed macrophages transfected with the miR-34c-3p mimic (Am) downregulate both *prkar2b* transcripts (left panel) and PRKAR2B protein levels (middle panel). **A right panel**. Reflecting greater *prkar2b* expression in attenuated macrophages *prkar2b*-luciferase activity is also higher in attenuated than virulent macrophages. Luciferase activity decreases when attenuated macrophages are transfected with the miR-34c-3p mimic (Am), decreases in virulent macrophages (V) and non-infected B cells (BL20), while overexpression of miR-34c-3p in attenuated macrophages decreases activity (A) (right panel). **B**. *T. annulata*-infected virulent macrophages (V) have higher PKA activity than attenuated (A) macrophages and overexpression of miR-34c-3p restores PKA activity in attenuated macrophages (left panel). Overexpression of miR-34c-3p in attenuated macrophages increases CREB-transactivation levels (right panel). Data represent mean ±SEM. n=3. ***P < 0.001 compared to V; ###P < 0.001 compared to A

Figure 3: miR-34c-3p levels impact on dissemination of *T. annulata*-transformed macrophages. The ability of virulent macrophages (V) to migrate in Matrigel is higher compared to attenuated macrophages (A). Overexpression of miR-34c-3p in attenuated macrophages (Am) restores Matrigel traversal to virulent macrophage (V) levels. Data represent mean ±SEM. ***$P < 0.001$ compared to V and ### $P<0.001$ compared to A.

Figure 4: miR-34c-3p targets both *prkar2b* and *Pfpkar* to regulate infected erythrocyte PKA activity independently of fluxes in cAMP. **A. Left panel.** miR-34c-3p levels drastically increase in infected red blood cells (iRBC) compared to noninfected (RBC)**,** specifically in merozoites (M), whereas it's nearly undetectable in schizonts (S) **(right panel). B**. **Left panel.** iRBC treated with the miR-34c-3p inhibitor increased both host and parasite Pf*pka-r* (right panel). Data represent mean ±SEM. n=3. R stands for rings and T for trophozoites. Data represent mean ±SEM. n=3. **$P < 0.005$ and ***$P < 0.001$.

Figure 5: Inhibition of miR-34c-3p increases infected erythrocyte PKA kinase activity and slows parasite development. A. iRBC display higher PKA activity as opposed to non-infected RBC. Inhibition of miR-34c-3p in iRBC (iRBCi) decreases their PKA activity. **B**. Parasites cultured for 64 h in untreated iRBCs are at ring and schizonts stages, but iRBC treated with the miR-34c-3p inhibitor harbor mainly schizont-stage parasites. In contrast to non-treated iRBC, rings and trophozoites were detected at 72 h and 93 h, respectively. **C**. Inhibition of miR-34c-3p reduces invasion of *Plasmodium*-infected RBC, whereas no adverse effect was observed when treated with the miR-155 inhibitor. D. Over expression of PfPKAr reduced the adverse effect of treatment with the miR-34c-3p mimic. R stands for rings, ET& LT for early and late trophozoites

and ES & LS for early and late schizonts. Data represent mean ±SEM. *n*=3. **P* < 0.05; ***P*< 0.005; ****P*< 0.001 ### *P*<0.001.

Supporting information:

Table S1: List of genes harboring miR-34c-3p seed sequences of whose transcription is upregulated in attenuated macrophages.

Figure S1: Alignment of pfpkar ortholog gene sequences from Haemosporidia and Piroplasm. The location of the incomplete miR-34c-3p seed in P. falciparum (pfal) is highlighted by the blue box.

Figure S2: FACS gating strategy for identification of parasite life cycle stages using SYBR green staining.

Figure S3: Alignment of PfPKAr ortholog protein sequences from Apicomplexa.

Figure S4: miR-34 and prkar2b expression levels in a human cancer cell lines (HL60 & HCT116) and adipose tissues. A. Overexpression of miR-34c-3p ablates PRAKR2B expression in HL60. B. BAT has higher levels of miR-34c and lower levels of PRAKR2B compared to WAT. Data represent mean ±SEM. n=3. ***P < 0.001.

A

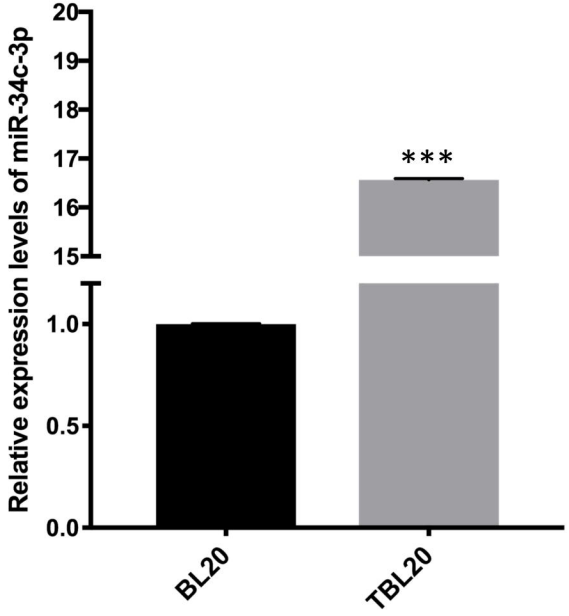
Relative expression levels of miR-34c-3p
20
19
18
17
16
15
1.0
0.5
0.0
***
BL20
TBL20

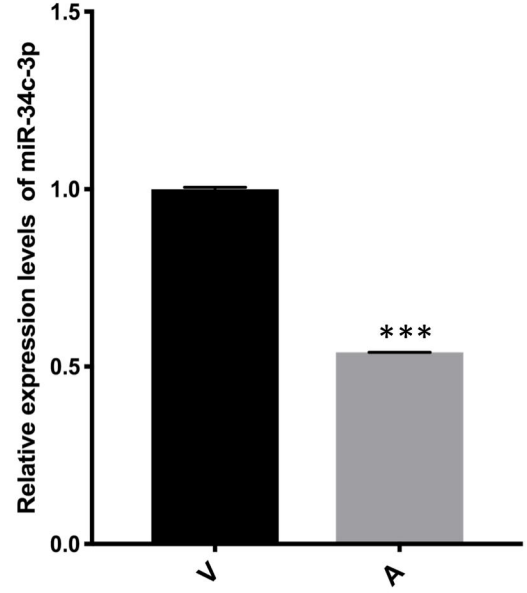
Relative expression levels of miR-34c-3p
1.5
1.0
0.5
0.0
***
V
A

B

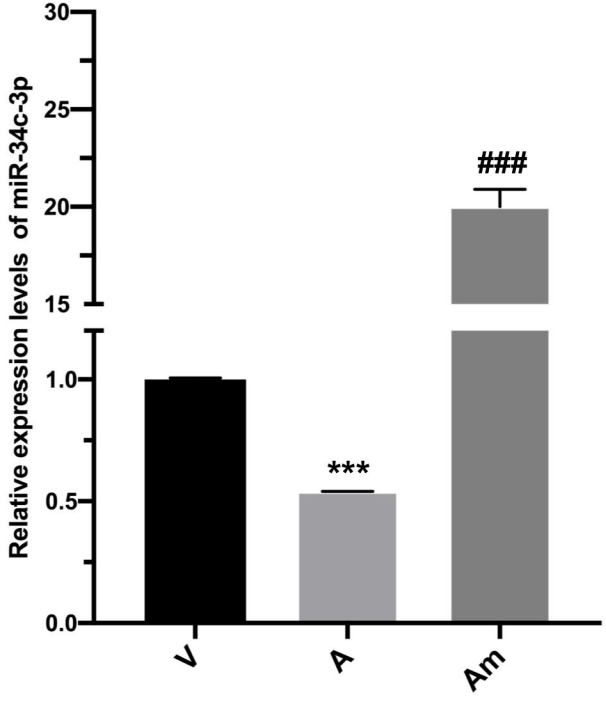
Relative expression levels of miR-34c-3p
30
25
20
15
1.0
0.5
0.0
***
###
V
A
Am

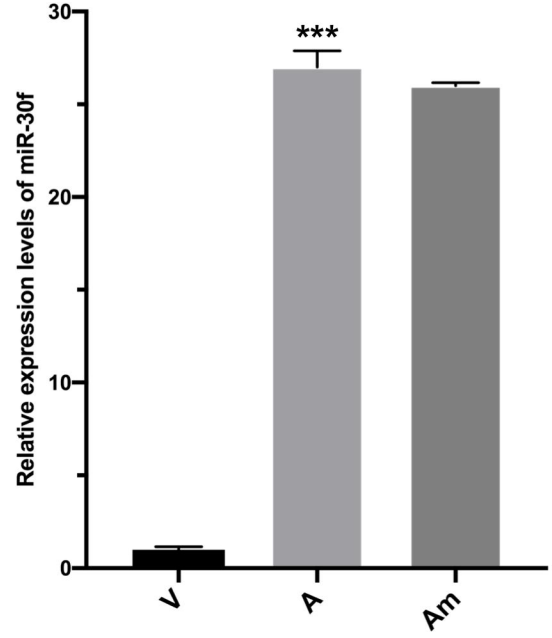
Relative expression levels of miR-30f
30
20
10
0
***
V
A
Am

A

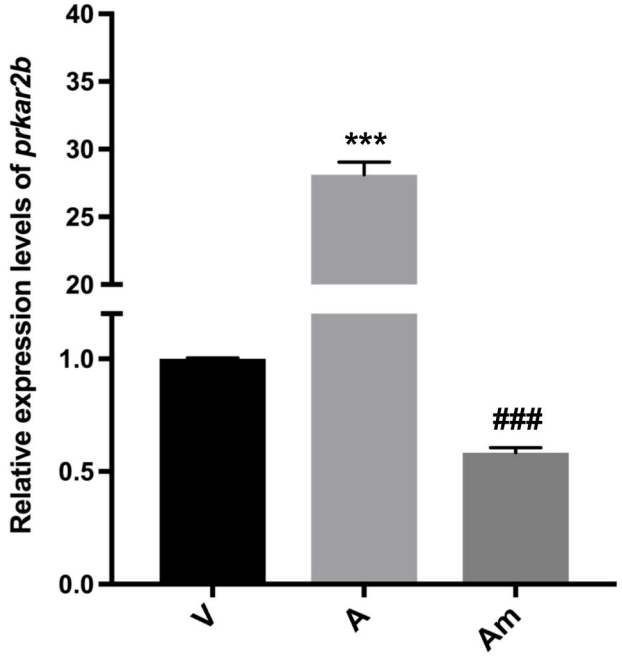
Relative expression levels of prkar2b
40
35
30
25
20
1.0
0.5
0.0
***
###
V
A
Am

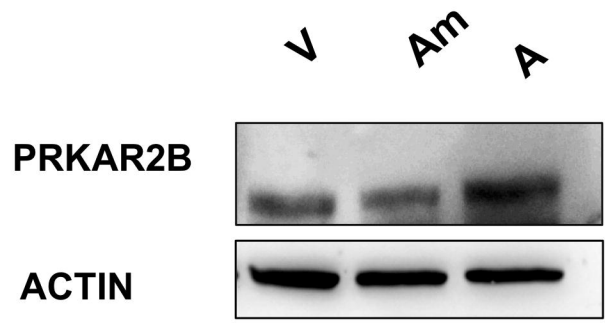
V
Am
A
PRKAR2B
ACTIN

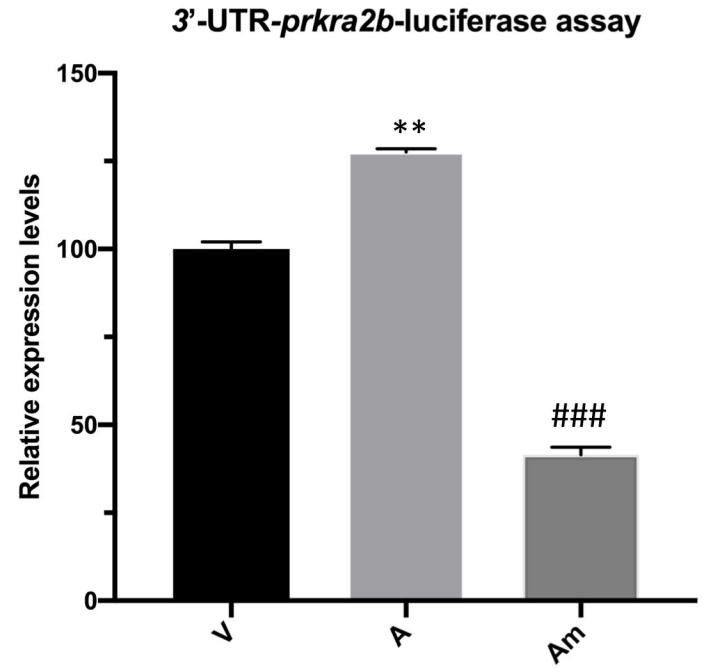
3'-UTR-prkra2b-luciferase assay
Relative expression levels
150
100
50
0
**
###
V
A
Am

B

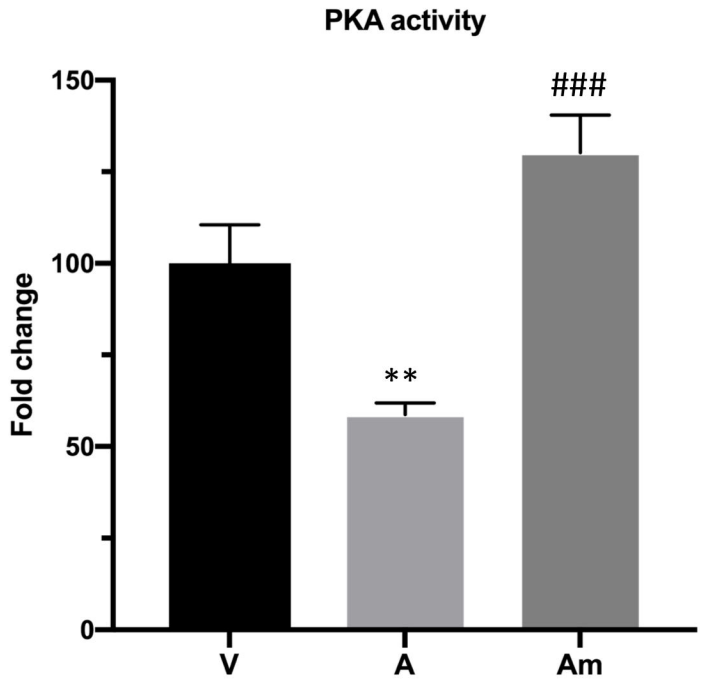
PKA activity
Fold change
150
100
50
0
**
###
V
A
Am

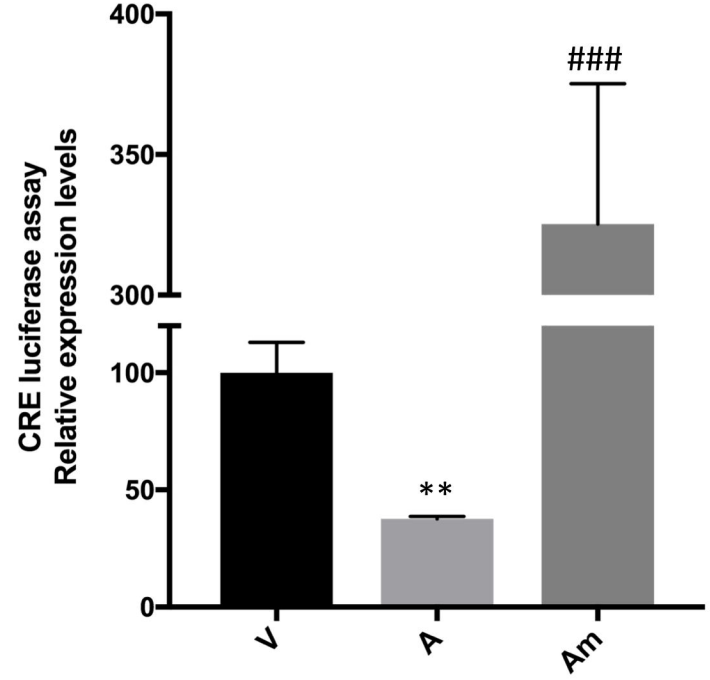
CRE luciferase assay
Relative expression levels
400
350
300
100
50
0
**
###
V
A
Am

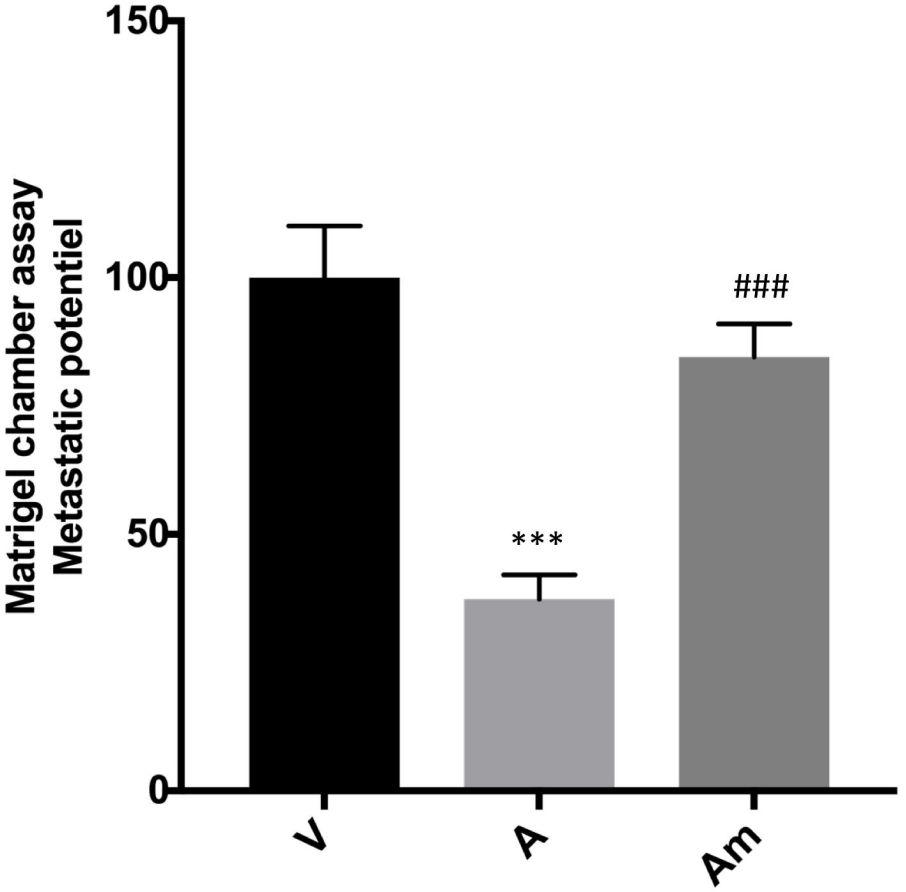
Matrigel chamber assay
Metastatic potentiel
150
100
50
0
***
###
V
A
Am

A

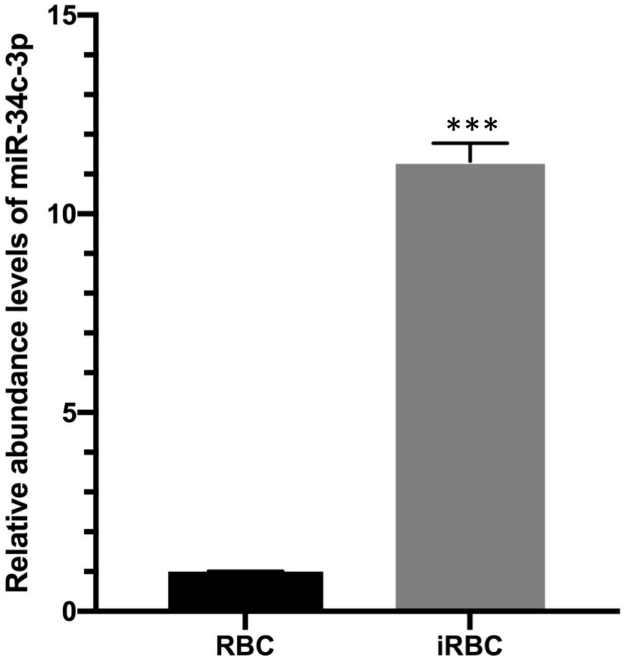
Relative abundance levels of miR-34c-3p
15
10
5
0
***
RBC
iRBC

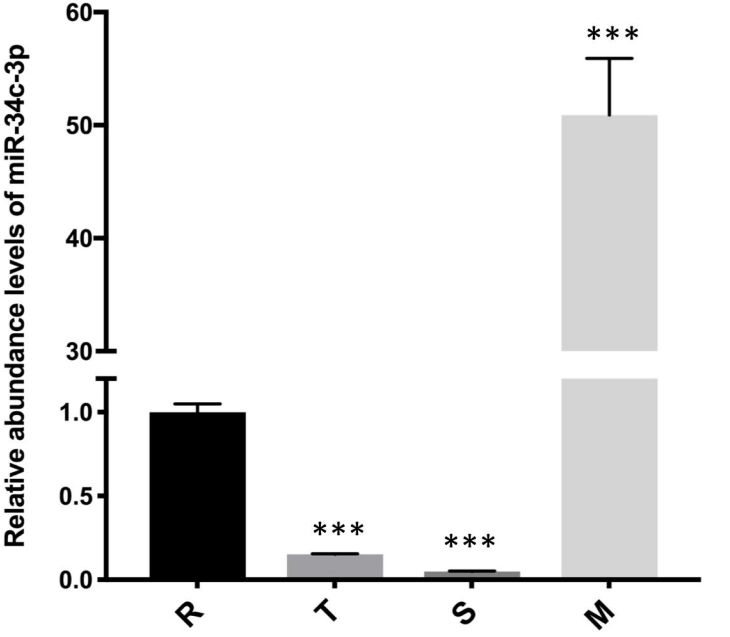
Relative abundance levels of miR-34c-3p
60
50
40
30
1.0
0.5
0.0
***
***
***
R
T
S
M

B

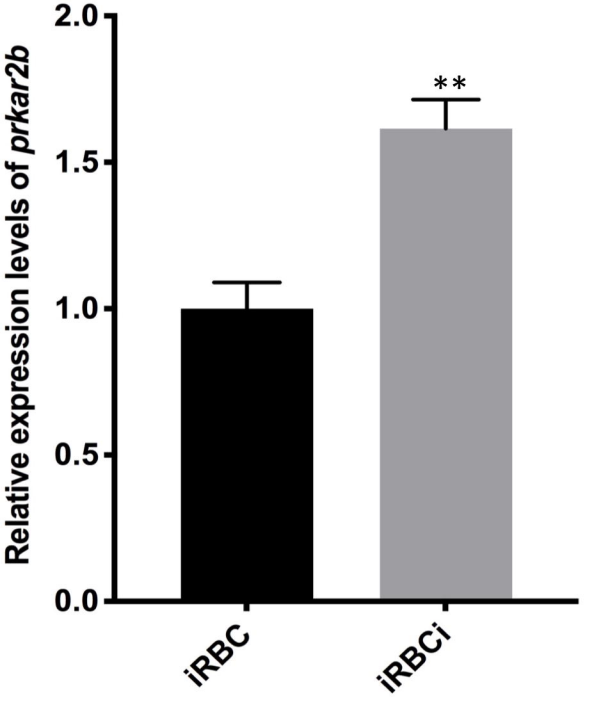
Relative expression levels of prkar2b
2.0
1.5
1.0
0.5
0.0
**
iRBC
iRBCi

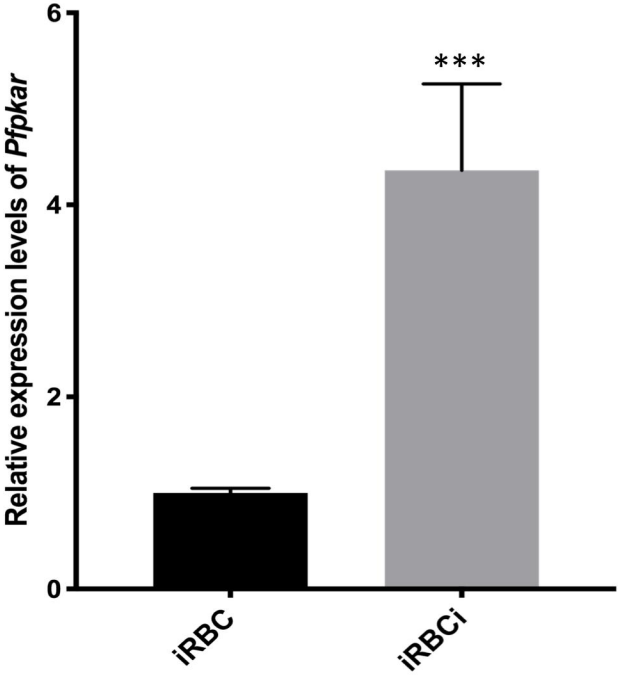
Relative expression levels of Pfpkar
6
4
2
0
***
iRBC
iRBCi

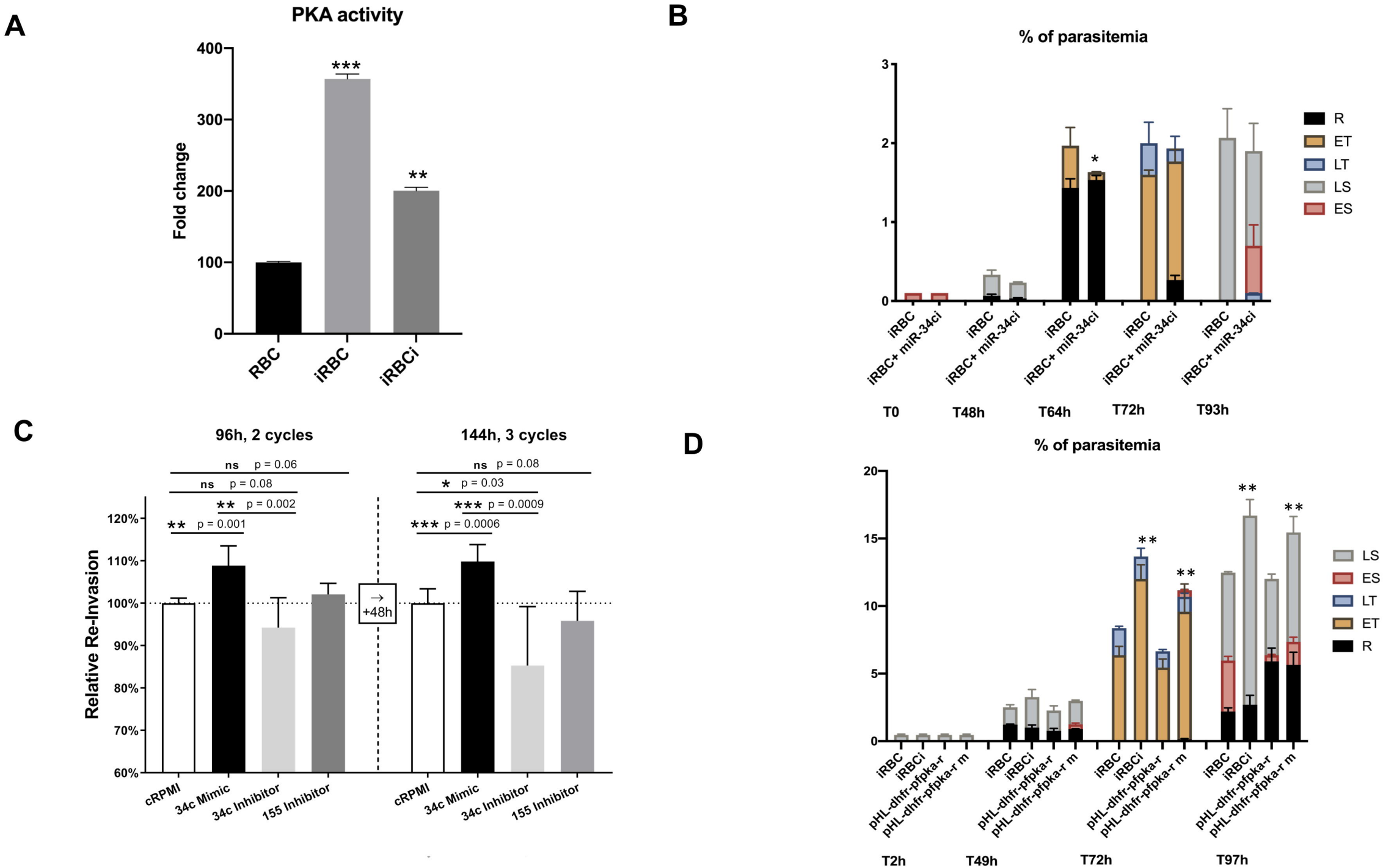
A
PKA activity
Fold change
400
300
200
100
0
***
**
RBC
iRBC
iRBCi
B
% of parasitemia
3
2
1
0
*
R
ET
LT
LS
ES
iRBC
iRBC+ miR-34ci
T0
T48h
T64h
T72h
T93h
C
96h, 2 cycles
144h, 3 cycles
ns p = 0.06
ns p = 0.08
** p = 0.002
** p = 0.001
ns p = 0.08
* p = 0.03
*** p = 0.0009
*** p = 0.0006
Relative Re-Invasion
120%
110%
100%
90%
80%
70%
60%
→ +48h
cRPMI
34c Mimic
34c Inhibitor
155 Inhibitor
D
% of parasitemia
20
15
10
5
0
**
LS
ES
LT
ET
R
iRBC
iRBCi
pHL-dhfr-pfpka-r
pHL-dhfr-pfpka-r m
T2h
T49h
T72h
T97h

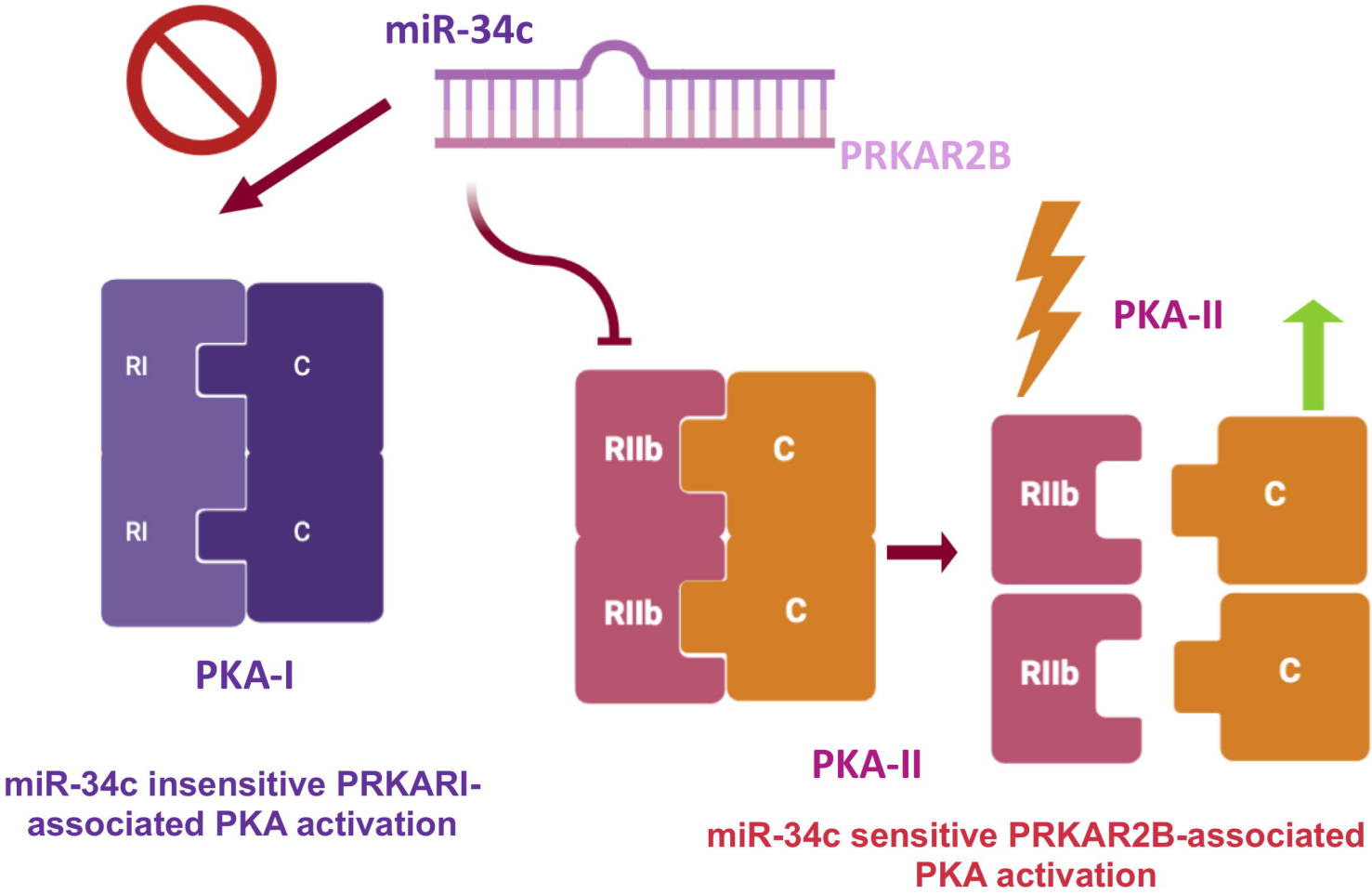

Mamalian PKA complexes